Heralded entanglement between widely separated atoms

Julian Hofmann[1], Michael Krug[1], Norbert Ortegel[1], Lea Gérard[1], Markus Weber[1*], Wenjamin Rosenfeld[1,2*], Harald Weinfurter[1,2]

[1]Fakultät für Physik, Ludwig-Maximilians-Universität München, D-80799 München, Germany
[2]Max-Planck Institut für Quantenoptik, D-85748 Garching, Germany

[*]To whom correspondence should be addressed: w.r@lmu.de; markusweber@lmu.de

Entanglement is the essential feature of quantum mechanics. Remarkably, observers of two or more entangled particles will find correlations in their measurement results, that can not be explained by classical statistics. To make it a useful resource, particularly for scalable long-distance quantum communication, the heralded generation of entanglement between distant massive quantum systems is necessary. We report on the creation and analysis of heralded entanglement between spins of two single Rb-87 atoms trapped independently 20 meters apart. Our results illustrate the viability of an integral resource for quantum information science, as well as for fundamental tests of quantum mechanics.

Entanglement between distant stationary quantum systems will be a key resource for future applications in the field of long-distance quantum communication, like quantum repeaters (*1*) and quantum networks (*2*). At the same time, it is an essential ingredient for new experiments on the foundations of physics, in particular for a first loophole-free test of Bell's inequality (*3–5*). Central to all these applications is the heralded generation of entanglement, i.e., a signal is provided once an entangled pair is successfully prepared.

Up to now, (unheralded) entanglement between separated massive quantum objects has been achieved for various systems (*6, 7*), even over $21\,\mathrm{m}$ (*8*). Heralded entanglement has been demonstrated with cold atomic ensembles (*9,10*), single trapped ions (*11,12*) and diamond crystals (*13*), albeit over short distances in a single setup only. For the realization of heralded entanglement over long distances single neutral atoms are promising candidates. In view of future applications, several important milestones have already been demonstrated for such systems: manipulation of atomic quantum registers (*14*), storage of quantum-information (*8,15–17*), fast

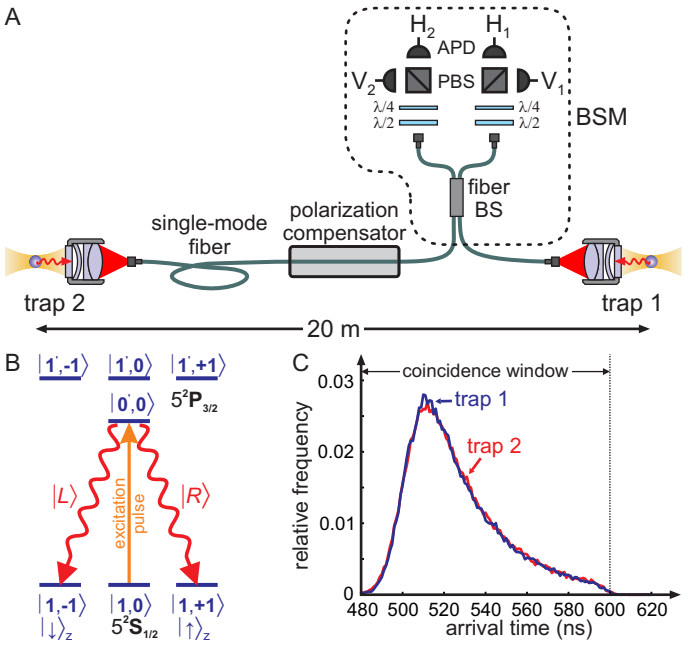

Figure 1: (A) Experimental setting: two independent single atom traps, operated in separate laboratories. Single photons emitted by the atoms interfere on a 50-50 fiber beam splitter (fiber BS) and are detected by avalanche photodiodes (APDs) behind a polarization analyzer consisting of half- and quarterwave plates ($\lambda/2$ and $\lambda/4$) and polarizing beam splitters (PBS). Simultaneous detection of two photons in particular combinations of detectors constitutes a Bell state measurement (BSM) on the photons and heralds the generation of entanglement between the separated atoms. (B) Scheme for generation of single photons whose polarization is entangled with the atomic spin. (C) Histograms of arrival times of the single photons from trap 1 (blue) and trap 2 (red). The photonic wave-packets are overlapped by synchronizing the two excitation procedures to better than $500\,\mathrm{ps}$.

and highly efficient state analysis (*18*), deterministic quantum gates between nearby trapped atoms via Rydberg-blockade (*19, 20*), and distribution of light-matter entanglement over large distances (*21*).

We report on the preparation and analysis of heralded entanglement between two single ^{87}Rb atoms over a distance of $20\,\mathrm{m}$ via entanglement swapping (*22*). The scheme starts with entangling the spin of each of the two atoms with the polarization state of a spontaneously emitted photon (*23*). The photons are guided to a Bell state measurement setup (BSM) where the two-photon polarization state is projected onto an entangled state, thereby providing the heralding signal. In a final step we evaluate the entanglement between the atomic spins.

Our experimental arrangement (Fig. 1A) consists of two independently operated experiments, here called trap 1 and trap 2 (*24*), which are situated in two laboratories and equipped with their own laser and control systems. In each experiment we load a single ^{87}Rb atom into

an optical dipole trap (*25*). The typical lifetime of a single trapped atom is $5 - 10\,\mathrm{s}$, limited mainly by heating during the experimental process and collisions with background gas. Photons emitted by the atoms are coupled into single-mode optical fibers and guided to the BSM-arrangement next to trap 1. The lengths of the optical fibers from trap 1 and trap 2 to the BSM are $5\,\mathrm{m}$ and $30\,\mathrm{m}$, respectively. In order to compensate for polarization drifts induced by temperature changes and mechanical stress in the $30\,\mathrm{m}$ fiber, an automatic polarization stabilization (*21*) is used. The interferometric BSM arrangement consists of a 50-50 single-mode fiber beam splitter (BS) with polarizing beam splitters (PBS) in each of the output ports. Additional half- and quarterwave plates allow us to select the measurement basis for the BSM and the atom-photon entanglement measurements. Finally, photons are detected by 4 avalanche photodiodes (APDs).

First, we verify atom-photon entanglement in each experiment separately. The generation of an entangled atom-photon state starts by preparing the atom in the initial state $5^2S_{1/2}$, $|F = 1,\, m_F = 0\rangle$ (Fig. 1B) via optical pumping. Then the atom is excited to the state $5^2P_{3/2}$, $|F' = 0,\, m_{F'} = 0\rangle$ by a short optical pulse (FWHM pulse length $21\,\mathrm{ns}$). In the following spontaneous decay the polarization of a single photon emitted into the collection optics (defining the quantization axis z) is entangled with the atomic spin (*23*), yielding the state

$$|\Psi\rangle_{AP} = \frac{1}{\sqrt{2}}\left(|\downarrow\rangle_z |L\rangle + |\uparrow\rangle_z |R\rangle\right) = \frac{1}{\sqrt{2}}\left(|\downarrow\rangle_x |V\rangle + |\uparrow\rangle_x |H\rangle\right),$$

where $|L\rangle$, $|R\rangle$ denote the left- and right-circular and $|H\rangle$, $|V\rangle$ the horizontal and vertical linear polarization states of the photon. The atomic qubit is defined by the Zeeman states $|m_F = +1\rangle$ and $|m_F = -1\rangle$ of the ground level $5^2S_{1/2}$, $F = 1$ which we associate with spin orientations $|\uparrow\rangle_z$ and $|\downarrow\rangle_z$, respectively. Preparation and excitation of the atom is repeated until a photon is detected. Taking into account additional cooling periods required to counteract heating of the atom, the preparation and excitation of the atom can be performed 50×10^3 times per second. The overall efficiency for detecting the photon after an excitation in trap 1 (trap 2) is $\eta_1 = 0.9 \times 10^{-3}$ ($\eta_2 = 1.25 \times 10^{-3}$). These numbers include the excitation probability, the collection and coupling efficiencies as well as losses in the optics, and also the quantum efficiency of the photodetectors. Polarization analysis of the single photons is performed with the BSM arrangement, which also serves to monitor fluorescence of the atom inside the trap.

In order to evaluate atom-photon entanglement, conditioned on the detection of the emitted photon the internal spin state of the atom is read out (*23*). The detection process consists of a Zeeman state-selective stimulated Raman adiabatic passage (STIRAP) (*26*) with subsequent hyperfine state detection. This process can be considered as a projection of the atom onto the state $\cos(\gamma)\,|\uparrow\rangle_x + \sin(\gamma)\,|\downarrow\rangle_x$, where γ is the angle of linear polarization of the STIRAP pulse defining the measurement basis (the angle of the corresponding direction of the atomic spin is 2γ). In atom-photon correlation measurements we register event numbers $N_{SS'}^{(\gamma,\delta)}$, where $S, S' \in \{|\uparrow\rangle, |\downarrow\rangle\}$ are the eigenstates of the spin of the atom and the photon along their respective measurement directions defined by γ and δ. Figure 2 shows the resulting correlations between atomic spin and photon polarization measurements for both traps separately.

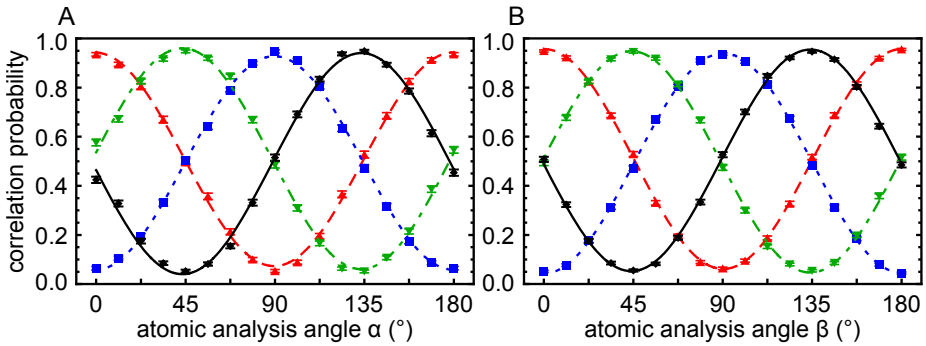

Figure 2: Atom-photon correlations for trap 1 (A) and trap 2 (B). The graphs show the measured correlation probabilities $\frac{1}{N}(N_{\uparrow\uparrow}^{(\gamma,0^\circ)} + N_{\downarrow\downarrow}^{(\gamma,0^\circ)})$ (red ▲ with dashed lines), $\frac{1}{N}(N_{\uparrow\uparrow}^{(\gamma,45^\circ)} + N_{\downarrow\downarrow}^{(\gamma,45^\circ)})$ (green ▼ with dot-dashed lines) and the anti-correlation probabilities $\frac{1}{N}(N_{\uparrow\downarrow}^{(\gamma,0^\circ)} + N_{\downarrow\uparrow}^{(\gamma,0^\circ)})$ (blue ■ with dotted lines) $\frac{1}{N}(N_{\uparrow\downarrow}^{(\gamma,45^\circ)} + N_{\downarrow\uparrow}^{(\gamma,45^\circ)})$ (black ♦ with solid lines), $\gamma \in \{\alpha, \beta\}$ as a function of the respective atomic analysis angle. Each point is deduced from $N = 1200 - 2400$ events, where N is the sum over the four possible measurement outcomes.

In these measurements the photon was detected in H/V basis ($\delta = 0^\circ$) and in $\pm 45^\circ$ basis ($\delta = 45^\circ$), while the atomic measurement angle α (trap 1) and β (trap 2) was varied between 0° and 180°. The visibilities $V^{(\delta)}$ of the correlation curves obtained by least-squares fits are $V_1^{(0^\circ)} = 0.869 \pm 0.006$, $V_1^{(45^\circ)} = 0.900 \pm 0.006$ for trap 1 and $V_2^{(0^\circ)} = 0.895 \pm 0.004$, $V_2^{(45^\circ)} = 0.901 \pm 0.005$ for trap 2, where the given errors are the expected statistical 1σ deviations. These high visibilities, limited mainly by the quality of the atomic state read-out, demonstrate that atom-photon entanglement is reliably generated and detected with high fidelity in both traps.

The second crucial condition for preparing a highly entangled state of two trapped atoms is a high-fidelity Bell-state measurement of the photons, i.e., projecting them onto maximally entangled states. We use interferometric Bell-state analysis based on the Hong-Ou-Mandel effect (*27*). This two-photon detection scheme does not require interferometric stability on a wavelength scale, thereby relaxing the experimental requirements for long-distance quantum communication. In general, at a beam-splitter, bunching (anti-bunching) of two photons in a symmetric (anti-symmetric) state enables one to identify Bell-states. In our case a coincidence in detectors H_1V_1 or H_2V_2 (Fig. 1A) signals projection of the photons onto the state $|\Psi^+\rangle_{Ph} = \frac{1}{\sqrt{2}}(|H\rangle|V\rangle + |V\rangle|H\rangle)$, and the coincidences H_1V_2 or H_2V_1 indicate projection onto the state $|\Psi^-\rangle_{Ph} = \frac{1}{\sqrt{2}}(|H\rangle|V\rangle - |V\rangle|H\rangle)$, respectively. The other two symmetric Bell-states $|\Phi^\pm\rangle_{Ph} = \frac{1}{\sqrt{2}}(|H\rangle|H\rangle \pm |V\rangle|V\rangle)$ give yet a different result but can not be distinguished from each other (*28–30*). Thus, by detecting one of the four coincidences mentioned above, we project the incoming photons unambiguously on a Bell-state, thereby heralding the generation of entanglement between the separated atoms.

The visibility of the two-photon interference, which determines the fidelity of the Bell-state

measurement, depends crucially on temporal, spatial and spectral indistinguishability of the arriving photons. Experimentally the temporal overlap is achieved by synchronizing the two excitation procedures in trap 1 and trap 2 to better than $500\,\mathrm{ps}$, which is far below the lifetime of the excited atomic state of $26.2\,\mathrm{ns}$, and by exactly matching the shapes of the interfering wave-packets (Fig. 1C). The single-mode fiber beam-splitter guarantees spatial mode overlap of unity. Frequency differences of the emitted photons are minimized by zeroing all relevant fields (*31*). Further reduction of the fidelity of the Bell-state measurement arises from two-photon emission by a single atom due to off-resonant excitation of the atom to the $5^2P_{3/2}$, $F' = 1$ level (see Fig. 1B, fig. S1) if the first photon is emitted already within the duration of the excitation pulse. However, due to the structure of the involved atomic levels, with a probability of 78.1% a polarization-entangled state $\frac{1}{\sqrt{2}}(|H\rangle_1 |H\rangle_2 + |V\rangle_1 |V\rangle_2)$ of the two consecutively emitted photons is formed (*32*). These events are registered as coincidences H_1H_2 and V_1V_2 and do not herald projection onto a Bell state. Reduction of the fidelity is therefore due to the remaining two-photon emissions and due to dark counts of the detectors. Based on additional calibration measurements we estimate a fidelity of the Bell-state projection of at least 92% (*32*).

By combining all methods described above we are able to generate and characterize entanglement between two distant atoms. In each of the two experiments a single atom is captured and the atom-photon entangling sequences are repeated until two photons are detected within a time-window of $120\,\mathrm{ns}$ in the BSM arrangement. With a coincidence probability of 0.54×10^{-6}, a repetition rate of $50\,\mathrm{kHz}$, and by taking into account the fraction of time when an atom was present in each of the traps of 0.35 we arrive at an atom-atom entanglement rate of about $1/106\,\mathrm{s}^{-1}$. A valid twofold detection, i.e., registration of $|\Psi^{\pm}\rangle_{Ph}$, heralds projection of the atoms onto the state $|\Psi^{\pm}\rangle_{AA} = \frac{1}{\sqrt{2}}(|\uparrow\rangle_x |\downarrow\rangle_x \pm |\downarrow\rangle_x |\uparrow\rangle_x)$. Subsequently, measurements of the atomic states are performed $1.2\,\mu\mathrm{s}$ (trap 1) and $0.95\,\mu\mathrm{s}$ (trap 2) after the coincidence detection (fig. S2). These times are far below the coherence time of the single atomic qubit state of $\tau_c = 75\,\mu\mathrm{s}$ (*17*) and the coherence time of the entangled atom-atom state, which we expect to be at least $\tau_c/2$, and thus does not limit the quality of our experiment (agreeably, the atom-atom entanglement rate and τ_c need substantial improvement for future quantum repeater scenarios).

To evaluate the atom-atom entanglement we perform measurements of the atomic spins in two bases. We have chosen analysis angles $\alpha = 90°$ and $\alpha = 135°$, while β is varied in steps of $22.5°$ between $90°$ and $180°$, or between $45°$ and $135°$, respectively. The obtained correlations are shown for the detection of the photonic $|\Psi^-\rangle_{Ph}$ state (Figs. 3A, B) and for the $|\Psi^+\rangle_{Ph}$ state (Figs. 3C, D). By fitting sinusoidal functions to the data points we obtain visibilities $V^{(\alpha)}$ of $V_{\Psi^-}^{(90°)} = 0.788 \pm 0.031$, $V_{\Psi^-}^{(135°)} = 0.728 \pm 0.032$ for the $|\Psi^-\rangle_{AA}$ state and $V_{\Psi^+}^{(90°)} = 0.813 \pm 0.030$, $V_{\Psi^+}^{(135°)} = 0.723 \pm 0.034$ for the $|\Psi^+\rangle_{AA}$ state, respectively. For estimation of the fidelity we assume that the visibility in the third (unmeasured) conjugate basis is equal to the lower of the two measured ones, arriving at $F_{\Psi^-} = 0.811 \pm 0.028$ and $F_{\Psi^+} = 0.815 \pm 0.028$. These numbers prove that in both cases an entangled state of the two atoms is generated. Moreover, the average visibilities $\bar{V}_{\Psi^\pm} = \frac{1}{2}(V_{\Psi^\pm}^{(90°)} + V_{\Psi^\pm}^{(135°)})$ of $\bar{V}_{\Psi^-} = 0.768 \pm 0.023$ and $\bar{V}_{\Psi^+} = 0.758 \pm 0.023$, respectively, are well above the threshold of 0.707 necessary to violate

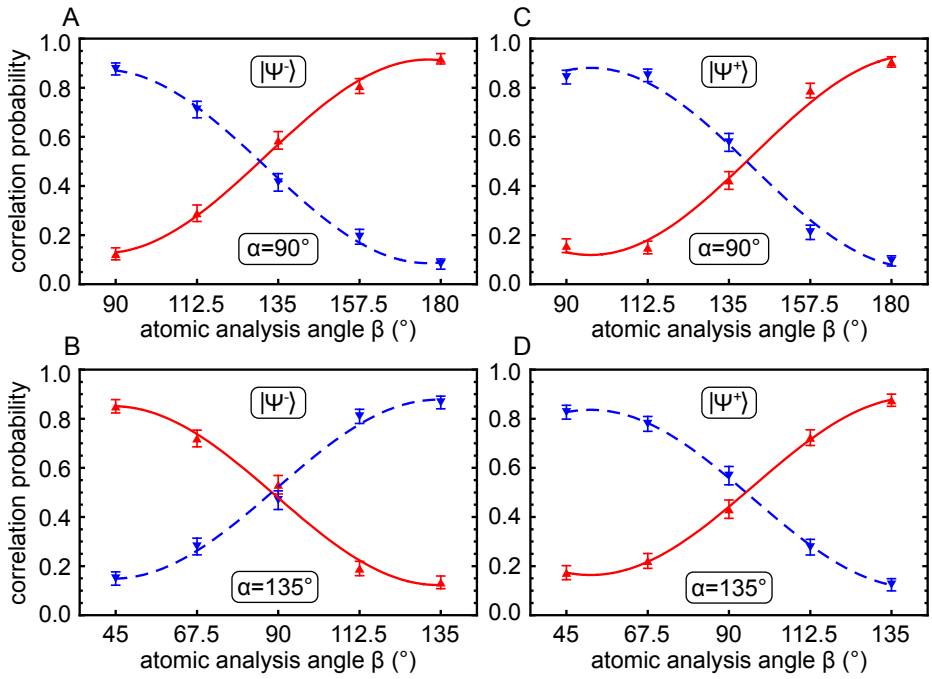

Figure 3: Atom-atom correlations obtained after Bell-state projection of the photons onto state $|\Psi^-\rangle_{Ph}$ (A,B) and $|\Psi^+\rangle_{Ph}$ (C,D), respectively. The measured correlation probabilities $\frac{1}{N}(N_{\uparrow\uparrow}^{(\alpha,\beta)} + N_{\downarrow\downarrow}^{(\alpha,\beta)})$ (red ▲ with solid lines), and the anti-correlation probabilities $\frac{1}{N}(N_{\uparrow\downarrow}^{(\alpha,\beta)} + N_{\downarrow\uparrow}^{(\alpha,\beta)})$ (blue ▼ with dashed lines) are shown for two complementary measurement bases. Each point is deduced from $N = 170 - 190$ atom-atom events. The overall number of events in this measurement is 3637, acquired within about 107 hours.

Bell's inequality.

One of our main goals is to enable a future loophole-free test of Bell's inequality (*3*). Inserting the data from the above measurements into $\langle\sigma_\alpha\sigma_\beta\rangle = \frac{1}{N}(N_{\uparrow\uparrow}^{(\alpha,\beta)} + N_{\downarrow\downarrow}^{(\alpha,\beta)} - N_{\uparrow\downarrow}^{(\alpha,\beta)} - N_{\downarrow\uparrow}^{(\alpha,\beta)})$ we evaluated the parameter $S = |\langle\sigma_\alpha\sigma_\beta\rangle + \langle\sigma_{\alpha'}\sigma_\beta\rangle| + |\langle\sigma_\alpha\sigma_{\beta'}\rangle - \langle\sigma_{\alpha'}\sigma_{\beta'}\rangle|$ from the Clauser-Horne-Shimony-Holt-inequality $S \leq 2$, which holds for local-realistic theories (*33*). For the data from Fig. 3, using the settings $\alpha = 135°$, $\beta = 67.5°$; $\alpha = 135°$, $\beta' = 112.5°$; $\alpha' = 90°$, $\beta' = 112.5°$ together with $\alpha' = 90°$, $\beta'' = 157.5°$ (replacing $\beta = 67.5°$), for all four heralding signals we obtain an S-value exceeding the limit of 2. Since a measurement result is obtained for each and every heralding signal, the average value of $S = 2.19 \pm 0.09$ for the first time yields definite violation without relying on the fair sampling assumption for a macroscopic distance.

Summarizing, in this experiment we demonstrated heralded entanglement between two atoms $20\,\mathrm{m}$ apart. It was high enough to violate a Bell-inequality, showing its suitability for quantum information applications such as device-independent quantum cryptography (*34*). The design of trap 2 allows rather straightforward extension of the distance between the two traps

to at least several hundred meters, limited only by transmission of photons in the optical fiber connection. Two distant entangled atoms form the elementary link of the quantum repeater, enabling efficient long-distance quantum communication. Together with efficient and fast atomic state detection (*18*), this experiment forms the basis for the first loophole-free Bell-experiment answering the longstanding question on whether a local realistic extension of quantum mechanics can be a valid description of nature.

References

1. H.-J. Briegel, W. Dür, J. I. Cirac, P. Zoller, *Phys. Rev. Lett.* **81**, 5932 (1998).
2. S. J. van Enk, J. I. Cirac, P. Zoller *Phys. Rev. Lett.* **78**, 4293 (1997).
3. J. F. Clauser, A. Shimony, *Rep. Prog. Phys.* **41**, 1881 (1978).
4. C. Simon, T. M. Irvine, *Phys. Rev. Lett.* **91**, 110405 (2003).
5. W. Rosenfeld *et al., Adv. Sci. Lett.* **2**, 469 (2009).
6. B. Julsgaard, A. Kozhekin, E. S. Polzik, *Nature* **413**, 400 (2001).
7. D. Matsukevich *et al., Phys. Rev. Lett.* **96**, 030405 (2006).
8. S. Ritter *et al., Nature* **484**, 195 (2012).
9. C. W. Chou *et al., Science* **316**, 1316 (2007).
10. Z. S. Yuan *et al., Nature* **454**, 1098 (2008).
11. D. L. Moehring *et al., Nature* **449**, 68 (2007).
12. D. N. Matsukevich, P. Maunz, D. L. Moehring, S. Olmschenck, C. Monroe, *Phys. Rev. Lett.* **100**, 150404 (2008).
13. K. Lee *et al., Science* **334**, 1253 (2011).
14. D. Schrader *et al., Phys. Rev. Lett.* **93**, 150501 (2004).
15. S. Kuhr *et al., Phys. Rev. Lett.* **91**, 213002 (2003).
16. H. Specht *et al., Nature* **473**, 190 (2011).
17. W. Rosenfeld, J. Volz, M. Weber, H. Weinfurter, *Phys. Rev. A* **84**, 022343 (2011).
18. F. Henkel *et al., Phys. Rev. Lett.* **105**, 253001 (2010).

19. T. Wilk *et al., Phys. Rev. Lett.* **104**, 010502 (2010).

20. L. Isenhower *et al., Phys. Rev. Lett.* **104**, 010503 (2010).

21. W. Rosenfeld *et al., Phys. Rev. Lett.* **101**, 260403 (2008).

22. M. Zukowski, A. Zeilinger, M. A. Horne, A. K. Ekert, *Phys. Rev. Lett.* **71**, 4287 (1993).

23. J. Volz *et al., Phys. Rev. Lett.* **96**, 030404 (2006).

24. M. Weber, J. Volz, K. Saucke, C. Kurtsiefer, H. Weinfurter, *Phys. Rev. A* **73**, 043406 (2006).

25. N. Schlosser, G. Reymond, P. Grangier, *Phys. Rev. Lett.* **89**, 023005 (2002).

26. F. Vewinger, M. Heinz, R.G. Fernandez, N. V. Vitanov, K. Bergmann, *Phys. Rev. Lett.* **91**, 213001 (2003).

27. C. K. Hong, Z. Y. Ou, L. Mandel, *Phys. Rev. Lett.* **59**, 2044 (1987).

28. H. Weinfurter, *Europhys. Lett.* **25**, 559 (1994).

29. K. Mattle, H. Weinfurter, P.G. Kwiat, A. Zeilinger, *Phys. Rev. Lett.* **76**, 4656 (1996).

30. S. L. Braunstein, A. Mann, *Phys. Rev. A* **51**, R1727 (1995).

31. W. Rosenfeld *et al., Optics and Spectroscopy* **111**, 535 (2011).

32. Materials and methods are available as supplementary material on *Science* Online.

33. J. F. Clauser, M. A. Horne, A. Shimony, R. A. Holt, *Phys. Rev. Lett.* **23**, 880 (1969).

34. A. Acin *et al., Phys. Rev. Lett.* **98**, 230501 (2007).

Acknowledgements

We thank A. Deeg, C. Jakob, and C. Kurtsiefer for help at the early stages of the experiment. This work was supported by the EU Project Q-Essence and the BMBF Project QuORep. J. H. acknowledges support by Elite Network of Bavaria through the excellence program QCCC.